The author wishes to acknowledge the helpful conversations with J. L. Johnson, D. J. Lees, and W. Millar.

*Work supported by the National Science Foundation under Grant No. GK-32131.

[1]P. Javel, W. Ohlendorf, G. W. Pacher, H. Pacher, and J. G. Wegrowe, Bull. Amer. Phys. Soc. 17, 1039 (1972).

[2]H. D. Pacher, C. Mahn, and G. Cattanei, Bull. Amer. Phys. Soc. 18, 1353 (1973).

[3]D. J. Lees, W. Millar, R. A. E. Bolton, G. Cattanei, and P. L. Plinate, in *Proceedings of the Fifth European Conference on Controlled Fusion and Plasma Physics, Grenoble, France, 1972* (Service d'Ionique Generale, Association EURATOM–Comissariat à l'Energie Atomique, Centre d'Etudes Nucléaires de Grenoble, Grenoble, France, 1972), Vol. II, p. 135.

[4]T. H. Stix, *The Theory of Plasma Waves* (McGraw-Hill, New York, 1962), p. 206.

[5]J. M. Dawson and M. Uman, Nucl. Fusion 5, 242 (1965).

[6]E. Cannobio, in *Proceedings of the Fourth European Conference on Controlled Fusion and Plasma Physics, Rome, Italy, 1970* (Comitato Nazionale per l'Energia Nucleare, Ufficio Edizioni Scientifiche, Rome, Italy, 1970), p. 101.

[7]Enhanced transport in TTMP due to parametric instabilities has been proposed by E. Cannobio at the Fifth International Conference on Plasma Physics and Controlled Nuclear Fusion Research, Tokyo, Japan, 11–15 November 1974. Another mechanism utilizing neoclassical transport theory including the effects of rf TTMP electric fields and the helical magnetic fields was proposed by T. E. Stringer at the Symposium on Plasma Heating in Toroidal Devices, Varenna, Italy, 1974.

[8]H. Grad, Phys. Fluids 10, 137 (1967).

[9]H. P. Furth and M. N. Rosenbluth, in *Plasma Physics and Controlled Nuclear Fusion Research* (International Atomic Energy Agency, Vienna, 1969), Vol. 1, p. 821.

[10]S. Fisher, H. Grad, Y. Sone, and J. Staples, in *Plasma Physics and Controlled Nuclear Fusion Research* (International Atomic Energy Agency, Vienna, 1969), Vol. 1, p. 899.

Stimulated Raman Scattering from Plasmas Irradiated by Normally and Obliquely Incident Laser Light

D. Biskamp and H. Welter
Max-Planck-Institut für Plasmaphysik, Garching, West Germany
(Received 15 October 1974)

The frequency spectrum and the angular distribution of the scattered light and the absorption coefficient due to stimulated Raman scattering are obtained by extensive numerical simulations of one- and two-dimensional plane plasma targets irradiated normally or obliquely by high-power laser light. Theoretical models are given to explain the numerical results.

Stimulated scattering of light from laser-irradiated plasmas has attracted much attention in recent years because of its detrimental influence on the laser-fusion concept. Stimulated Raman scattering (SRS) is due to parametric excitation of an electron plasma wave which coherently scatters off part of the laser intensity. Thresholds and growth rates for SRS have previously been computed for various conditions (see, for instance, Forslund, Kindel, and Lindman[1] and Galeev *et al.*[2]) and some important nonlinear properties have been found particularly from numerical simulations.[1,3] The present paper considerably extends previous theoretical understanding.

We first report numerical and theoretical results on the frequency spectrum of the scattered light and the process of dissipation due to SRS. The computed system, one-dimensional in space with transmitting boundary conditions, has a linear density profile with $n_{max}=n_c/2$, an inhomogeneity scale $L\equiv n(dn/dx)^{-1}=50c/\omega_0$ at $n=n_c/4$, and an initial electron temperature $T_{e0}/m_ec^2=10^{-3}$. As in all simulations of SRS the ions are assumed immobile. Electrons hitting the boundary on the dense side of the system are absorbed and reemitted cool to simulate a net heat flow out of the system and allow a quasistationary nonlinear state to be established.

For laser amplitudes $0.06\lesssim v_0/c\leq 0.1$, $v_0\equiv eE_0/m_e\omega_0$, $\vec{E}_0=E_0\vec{e}_0\cos(\vec{k}_0\cdot\vec{x}-\omega_0 t)$, a plasma wave train is excited and is localized at $n\simeq n_c/4$ with

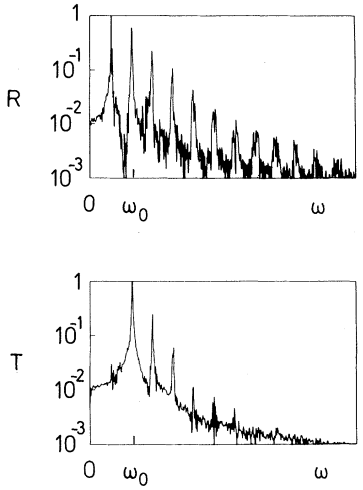

FIG. 1. Frequency spectra of the reflected and the transmitted light, $R(\omega)$ and $T(\omega)$ (logarithmic scale) for nondissipative SRS from a one-dimensional simulation with $v_0/c = 0.1$.

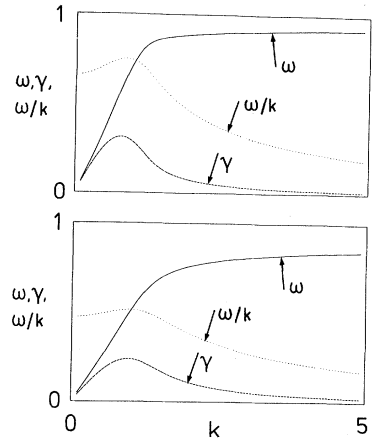

FIG. 2. Solution of the dispersion relation for a model distribution f_e, consisting of a bulk (δ function at $v = 0$) term and a linearly decreasing tail, containing 10% of the electrons (upper diagram) and 20% of the electrons (lower diagram). Velocity and frequency are normalized to the maximum tail velocity and the total plasma frequency. For large k, ω approaches the plasma frequency of the bulk density.

$\omega = \omega_{pe} = \omega_0/2$. Light absorption is weak in this intensity regime. A remarkable feature is the appearance of a spectrum of anti-Stokes lines in both the transmitted and the reflected light, Fig. 1, with a regular line spacing $\Delta\omega = \omega_{pe}$. The effect can be described by the following model equation, valid for not too large amplitudes:

$$\frac{\partial^2 A^{(n)}}{\partial t^2} - c^2 \frac{\partial^2 A^{(n)}}{\partial x^2} + \omega_{pe}^2 A^{(n)} = -\omega_{pe}^2 \frac{\tilde{n}}{n} A^{(n-1)}, \quad (1)$$

where $A^{(n)}$ is the vector potential of the nth order spectral line. Here $\tilde{n}$ is a finite-amplitude plasma wave packet with frequency ω_{pe} and a sufficiently small spatial width since phase matching for this process cannot be satisfied exactly in one dimension. For anti-Stokes frequencies in the transmitted light the coupling described by Eq. (1) is efficient (approximate phase matching) if $\tilde{n}$ has phase velocity along the density gradient as generated directly by SRS. Production of anti-Stokes lines in the reflected light, however, requires a component of $\tilde{n}$ with phase velocity opposite to the density gradient. This is also found when solving Eq. (1) numerically. Such outbound plasma waves are not excited by the fundamental Raman process, but are generated by reflection of inbound plasma waves at their cutoff slightly above $n_c/4$. The presence of outbound modes is clearly observed in the simulations.

For laser intensities $v_0/c > 0.1$, strong absorption and electron heating occur and determine the saturation of the parametric instability, mode-coupling effects such as the production of anti-Stokes lines being weak. A rather turbulent field of electron-density oscillations is excited extending beyond $n_c/4$. Electron heating is connected with the formation of a high-energy tail in $f_e(v_x)$. Although this is a strongly nonlinear effect, the main features of the quasistationary state of light reflection and absorption and electron heat conduction may be described by a quasilinear approach, where the frequency and damping rate of the plasma oscillations are determined by the linear dispersion properties due to the distribution f_e including the tail. Since the tail extends beyond the phase velocities of the electrostatic modes excited, the dispersion relation for these modes is changed and contains a new beam-like branch. Figure 2 shows frequency, damping rate, and phase velocity of this branch for an appropriate model distribution. Since the frequency is considerably smaller than the plasma frequency, in particular at the point of maximum damping, plasma oscillations are excited by SRS at $n > n_c/4$. There is also a decrease in phase velocity with increasing strength of the tail. In a self-consistent system this should lead to a reduction of the maximum tail velocity as is in fact observed in the simulations; see Fig. 3.

Figure 3 also shows the blue shift of the Raman frequency ω_1 because of the reduction of $\omega = \omega_0$

TABLE I. Reflectivity R, transmission coefficient T, absorption coefficient A, and frequency of the plasma modes ω/ω_0 for two runs, $v_0/c=0.2$ and 0.3. $(\omega/\omega_0)_{theor}$ is obtained from Eq. (2); $(\omega/\omega_0)_{exp}$ by measuring $\omega_0-\omega_1$ in the frequency spectrum of the reflected light, as shown in Fig. 3.

v_0/c	R	T	A	$(\omega/\omega_0)_{theor}$	$(\omega/\omega_0)_{exp}$
0.2	0.43	0.27	0.30	0.40	0.41
0.3	0.41	0.43	0.16	0.28	0.30

$-\omega_1$ predicted by the modified dispersion relation. Comparing the observed values of ω with the dispersion curves of Fig. 2 where the model distributions have about the same tail population (10% and 20%, respectively) as the distributions shown in Fig. 3, we find approximate agreement with the values of ω at the point of maximum damping. This is in the spirit of a quasilinear saturation where the modes most strongly driven by SRS require the largest damping rates. The Raman frequency ω_1 and the absorption coefficient A are connected by a relation derived from the Manley-Rowe relations for a three-wave parametric process.[4] With introduction of the reflection coefficient R and the transmission coefficient T such that $A=1-R-T$, it is found that

$$A=[(\omega_0-\omega_1)/\omega_0](1-T). \tag{2}$$

The values of ω_1 obtained from the frequency spectra and those obtained from Eq. (2) with use of the observed values of A and T agree quite well, as seen in Table I. From Eq. (2), the *decrease* of A with increasing laser intensity in the dissipative regime $v_0/c \gtrsim 0.2$ is related to the reduction of the frequency ω of the electrostatic modes.

The angular distribution of the scattered Raman light is investigated by two-dimensional simulations. Here boundary conditions along the density gradient are identical to those used in the one-dimensional simulations while we apply periodicity in the transverse direction. A general numerical result is that SRS occurs mainly at those points of the density profile where $k_{1x}\simeq 0$, i.e., at the classical turning points of the scattered light (the localization of SRS at $n_c/4$ in the one-dimensional simulations is a special case of this phenomenon). To explain this behavior, we recall that, in an inhomogeneous plasma, parametric instabilities are in general convective.[5] Only at particular points may absolute instabilities

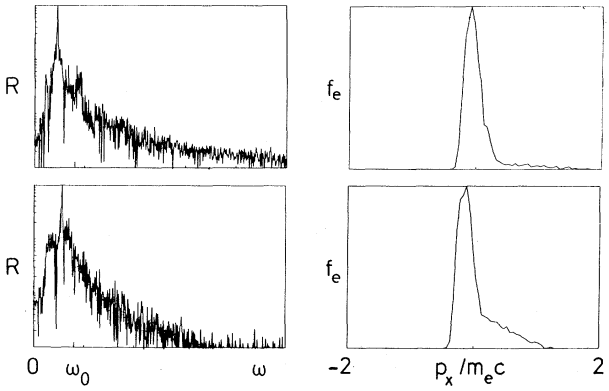

FIG. 3. Frequency spectra of the reflected light $R(\omega)$ and distribution functions $f_e(p_x)$ for dissipative SRS, from two one-dimensional simulations: $v_0/c=0.2$, upper figures; $v_0/c=0.3$, lower figures.

arise. For SRS it has been shown[6] that the Raman cutoff density $n_c/4$ is such a point. The results of Ref. 6 can be generalized to the case of side scattering ($k_{1y}\neq 0$) and oblique incidence ($k_{0y}\neq 0$).[7] In the limit $\gamma \ll \gamma_0$, γ_0 the homogeneous growth rate, the most interesting case for applications, the wave equation for the vector potential of the scattered wave becomes formally identical with the corresponding equation in Ref. 6,

$$c^2\frac{d^2A_1}{d\xi^2}+\left(\frac{L}{\omega_{pe}}\right)^2\left(\alpha^2+\frac{V^2-\gamma^2-\xi^2}{\xi}\right)A_1\simeq 0; \tag{3}$$

$$\xi=\omega_{pe}{}^2x/L,\quad L=n(dn/dx)^{-1},$$

$$V^2=\omega_{pe}{}^2\cos^2\varphi\, v_0{}^2k^2/4,\quad \alpha^2=\omega_1{}^2-k_{1y}{}^2c^2-\omega_{pe}{}^2,$$

$$\vec{k}=\vec{k}_0-\vec{k}_1,\quad \vec{A}_0\cdot\vec{A}_1=A_0A_1\cos\varphi.$$

Thus, in the limit $\gamma \ll \gamma_0$ the various side-scattering processes at $n<n_c/4$ differ from the scattering at $n_c/4$ only by different values of V^2 and $L/\omega_{pe}{}^2\propto L/n$, and hence correspond to the same absolute instability. The growth rate increases with increasing V^2 and L/n. As a function of density and angle of incidence θ_0, we have

$$V^2\propto\frac{n}{n_c}\left[2-2\left(\frac{n}{n_c}\right)^{1/2}-\frac{n}{n_c}-2k_{0y}k_{1y}\frac{c^2}{\omega_0{}^2}\right], \tag{4}$$

where $k_{0y}c/\omega_0=\sin\theta_0$, and $k_{1y}{}^2c^2/\omega_0{}^2=1-2(n/n_c)^{1/2}$.

To discuss the simulation results in more detail, it is convenient to distinguish between the polarization vector A_0 in or perpendicular to the plane of scattering (which is the plane of incidence for oblique incidence). Let us first consider the latter case. For normal incidence, $k_{0y}=0$ in Eq. (4), V^2 has a maximum at $n=n_c/4$, but

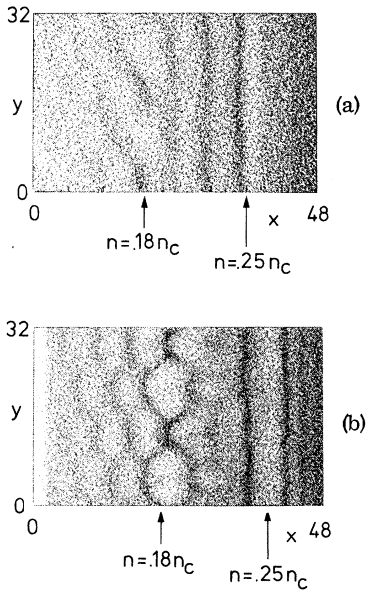

FIG. 4. Plots of simulation electrons from two-dimensional runs with normal incidence, $v_0/c=0.1$, $T_{e0}=10^{-3}m_ec^2$; x and y in units of c/ω_{pe}. (a) Linear density profile $n(x)=(0.2x/48+0.1)n_c$; (b) exponential profile $n(x)=0.3\exp[(x-48)/50]n_c$. The cell size in these runs is $\Delta x=\Delta y=0.5c/\omega_{pe}$, and the number of simulation electrons is approximately 5×10^4.

only slowly decreases with decreasing n. Thus, for a linear density profile, $L/n=$ const, there should be backscattering at $n_c/4$ and side scattering at some lower density with backscattering slightly dominating. This is, in fact, observed in the simulations; see Fig. 4. (Note that side scattering leads to scattered light outside the plasma propagating at some angle θ_1 because of refraction, $\tan\theta_1=k_{1y}/k_{1x}=\{[1-2(n/n_c)^{1/2}]n_c/n\}^{1/2}$.) For an exponential density slope, $L=$ const, however, scattering at some $n<n_c/4$ dominates because of the larger L/n. There seems to be the general tendency for a single mode to dominate at least in a finite region of the size of several wavelengths. Figure 4 gives an example of such behavior, where the modes $n_y=0$ at $n=0.25n_c$ and $n_y=2$ at $n=0.18n_c$ are excited while the mode $n_y=1$ at the intermediate density $n=0.23n_c$ is suppressed nonlinearily.

Oblique-incidence simulations show that SRS always takes place at some $n<n_c/4$. Side scattering with $k_{0y}k_{1y}<0$ dominates, thus leading to Raman light propagating back into the quadrant of incidence. The results can be explained by the theory outlined above. Given a density profile and an angle of incidence θ_0, the scattering mode with the largest growth rate can be computed in a straightforward way; e.g., for a linear profile and $\theta_0=23°$, $\gamma_{\max}=\gamma(n=0.2n_c)\simeq1.24\gamma(n=n_c/4)$. Thus in general the frequency ω_1 of the Raman light is higher than $\omega_0/2$ and SRS at $n_c/4$, as seen in the one-dimensional simulations, is found only under rather special conditions. However, the conclusions from these simulations, i.e., the generation of Raman anti-Stokes light and the process of the dissipation, are valid also in higher dimensions if suitably modified.

If the polarization vector is in the plane of scattering, SRS is found to be much weaker since $V^2\propto\cos^2\varphi$, while the $2\omega_{pe}$-decay instability is excited. For normal incidence, Raman backscattering at $n\simeq0.25n_c$ and the $2\omega_{pe}$ decay coexist but for oblique incidence the $2\omega_{pe}$ decay is the dominant process leading to considerable absorption of light. In this case the decay modes are strongly asymmetric, the outward-propagating plasma mode being much stronger than the inward-propagating one, creating a situation which is phenomenologically similar to resonant absorption at $n\simeq n_c$. A detailed theoretical analysis is still to be done. The decay process is also associated with some anomalous scattering of light ($\lesssim5\%$) at $\omega_0/2$ and $3\omega_0/2$, with the latter strongly dominating because of the predominance of the outward-going plasma mode. Thus the light at $3\omega_0/2$ recently observed experimentally[8,9] seems to be due to the $2\omega_{pe}$ decay and not to SRS which in those experiments has probably not been excited because of its high threshold.

In conclusion, we have presented simulation and theoretical results on stimulated Raman scattering in an inhomogeneous plasma concerning the frequency spectrum of the scattered light, the process of absorption, and the angular distribution of scattered light for general direction of incidence of the laser light. For polarization in the plane of incidence the $2\omega_{pe}$ decay is stronger than SRS and seems to be responsible for the half-harmonic frequencies, essentially $3\omega_0/2$, recently observed experimentally.

This work was performed under the terms of the agreement on association between the Max-Planck-Institut für Plasmaphysik and EURATOM.

[1]D. W. Forslund, J. M. Kindel, and E. L. Lindman, Phys. Rev. Lett. 30, 739 (1973).

[2]A. A. Galeev, G. Laval, T. M. O'Neil, M. N. Rosenbluth, and R. Z. Sagdeev, Pis'ma Zh. Eksp. Teor. Fiz. 17, 35 (1973) [JETP Lett. 17, 48 (1973)].

[3]H. H. Klein, W. M. Manheimer, and E. Ott, Phys. Rev. Lett. 31, 1187 (1973).
[4]W. H. Louisell, *Coupled Mode and Parametric Electronics* (Wiley, New York, 1960).
[5]M. N. Rosenbluth, Phys. Rev. Lett. 29, 565 (1972).
[6]J. F. Drake and Y. C. Lee, Phys. Rev. Lett. 31, 1197 (1973).
[7]Very recently a similar theoretical investigation has been performed by C. S. Liu, M. N. Rosenbluth, and R. B. White, Phys. Fluids 17, 1211 (1974).
[8]J. L. Bobin, M. Decroisette, B. Meyer, and Y. Vitel, Phys. Rev. Lett. 30, 594 (1973).
[9]P. Lee, D. V. Giovanelli, R. P. Godwin, and G. H. McCall, Appl. Phys. Lett. 24, 406 (1974).

Reflection of Phonons at Interfaces between Silicon and Solid Hydrogen and Deuterium*

Jay S. Buechner and Humphrey J. Maris
Department of Physics, Brown University, Providence, Rhode Island 02912
(Received 18 November 1974)

The reflection of phonons at an interface between a silicon crystal and solidified hydrogen and deuterium has been investigated by the heat-pulse method. The reflection coefficients are found to be much smaller than predicted by the acoustic-mismatch theory.

According to the theory of Khalatnikov,[1] the thermal boundary resistance (Kapitza resistance) at an interface between two materials occurs because phonons attempting to pass from one medium to the other are reflected by the mismatch in the acoustic properties of the media. Experimental investigations of the thermal boundary resistance[2] have traditionally measured either (1) the resistance at the interface between a classical solid (e.g., silicon or copper) and liquid ^{3}He or ^{4}He, or (2) the resistance between two classical solids. In experiments of type (1) a wide variety of solids has been investigated. In every case, the measured Kapitza resistance has been considerably smaller, by up to a factor of 100, than the value predicted by the acoustic-mismatch theory, except at very low temperatures ($T<0.1$°K). On the other hand, in experiments of type (2) involving two classical solids, the results have been in generally good agreement with the acoustic-mismatch theory. One could speculate, therefore, that the anomalously small value of the Kapitza resistance to liquid helium is an effect unique (a) to liquids, (b) to helium, or (c) to any material in which quantum effects are important. Folinsbee and Anderson[3] have shown that the Kapitza resistance to liquid and solid helium are of the same order of magnitude, indicating that speculation (a) is incorrect. To decide between (b) and (c) one must study a quantum system other than helium. A convenient measure of the importance of quantum effects is de Boer's "quantum parameter" Λ^*. Λ^* is defined by

$$\Lambda^* = h/\sigma(m\epsilon)^{1/2},$$

where σ and ϵ are the range and strength, respectively, of the interatomic potential, and m is the molecular mass. Materials for which $\Lambda^* \leq 0.5$ are classical in the sense that zero-point motion makes only a small correction to the lattice dynamics.[4] For ^{3}He and ^{4}He Λ^* is 3.08 and 2.68, respectively. The only other materials with $\Lambda^* > 1$ are H_2 and D_2, for which Λ^* has values 1.73 and 1.22. We report here measurements for these solids. In order to make a comparison, data were also taken for liquid and solid ^{4}He, and for solid neon ($\Lambda^* = 0.59$).

The experiments used the heat-pulse technique instead of the traditional dc-heat-flow Kapitza-resistance measurement. Using this method, one can study the reflection coefficient of phonons of a particular polarization, whereas the dc method averages over phonon polarizations. The experimental arrangement (Fig. 1) was similar to that of Guo and Maris.[5] The silicon crystal and sample chamber, surrounded by a vacuum space, were in thermal contact with a helium pot. The temperature was controlled by pumping on the pot and by varying the current through an attached resistance heater. At the beginning of the experiment the sample chamber A was under vacuum. A pulse of phonons was generated at the lower face of the silicon by Joule heating of a thin film of Constantan. Some of these phonons were reflected from the upper face of the silicon and detected by one of two thin-film superconducting bolometers on the lower face. Separate echoes were observed corresponding to longitudinal and transverse phonons, and also to phonons whose time of flight indicated that they had undergone

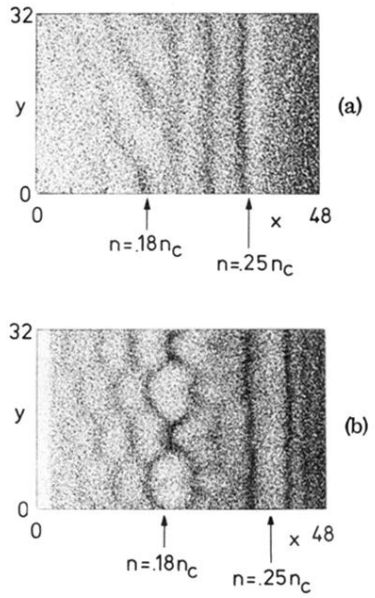

FIG. 4. Plots of simulation electrons from two-dimensional runs with normal incidence, $v_0/c = 0.1$, $T_{e0} = 10^{-3} m_e c^2$; x and y in units of c/ω_{pe}. (a) Linear density profile $n(x) = (0.2x/48 + 0.1)n_c$; (b) exponential profile $n(x) = 0.3 \exp[(x - 48)/50]n_c$. The cell size in these runs is $\Delta x = \Delta y = 0.5c/\omega_{pe}$, and the number of simulation electrons is approximately 5×10^4.